Int J Clin Exp Med 2015;8(1):1087-1093
www.ijcem.com /ISSN:1940-5901/IJCEM0003288

Original Article

A novel tissue-engineered bone in repairing femoral head defect and necrosis

Wuxun Peng[1], Lei Wang[1], Jian Zhang[1], Jin Deng[1], Yuekun Gong[2], Shihe Li[2], Yunyu Hu[3]

[1]Department of Emergency Surgery, Guiyang Medical College, Guiyang 550004, China; [2]The First Affiliated Hospital of Kunming Medical College, Kunming 650032, China; [3]Department of Orthopaedics, Xijing Hospital, The Fourth Military Medical University, Xi'an 710032, China

Received October 21, 2014; Accepted January 7, 2015; Epub January 15, 2015; Published January 30, 2015

Abstract: Objective: To evaluate the therapeutic effects of AACB/BMP/bFGF, a novel tissue-engineered bone, in repairing femoral head defect and necrosis in dog models. Methods: Dog models of avascular necrosis of femoral head (ANFH) were established by liquid nitrogen freezing method. Group A was untreated; Groups B, C, and D were implanted with AACB, AACB/BMP, and AACB/BMP/bFGF complex, respectively; Group E was grafted with autologous cancellous bone. Samples were collected at 3 w, 6 w, and 12 w after operation. A series of examinations were carried out to investigate the effects of the materials in repairing femoral head defect, including anatomical observation, X-ray examination, histological analysis, and vascular immunohistochemical staining. Results: Our results indicated that, compared with AACB alone and AACB/BMP, AACB/BMP/bFGF complex could exert the most efficient therapeutic effects in dog ANFH models. X-ray examination further confirmed that AACB/BMP/bFGF complex could effectively repair the injuries in dog ANFH models, almost to a comparable level with cancellous bone autografts. Moreover, histological analysis indicated that AACB/BMP/bFGF complex greatly enhanced the new bone formation, which would contribute to the healing of ANFH. Furthermore, vascular immunohistochemical staining revealed that AACB/BMP/bFGF complex could significantly stimulate the revascularization in defect areas, reflecting the post-injury healing process in these models. Conclusion: AACB/BMP/bFGF complex has great potential in repairing femoral head defect by enhancing osteogenesis and revascularization. The novel tissue-engineered bone would be widely used in clinical applications for ANFH treatment, especially as an alternative for autografts.

Keywords: Avascular necrosis of femoral head, basic fibroblast growth factor, bone morphogenetic protein, allogeneic antigen-extracted cancellous bone

Introduction

Avascular necrosis of the femoral head (ANFH) is one of the most common orthopedic diseases, and the treatment of the disease has always been a big challenge in clinic. With the development of tissue engineering, bone tissue engineering technique provides a promising tool to repair femoral head necrosis [1]. As is known to all, in tissue engineering strategies, the scaffold is a key component. Certain strength, easy to degrade, and minimized immunogenicity make excellent scaffold materials [2].

Polyvinylpyrrolidone (PVP) is a good carrier for growth factors [3, 4], and the surface of an allogeneic antigen-extracted cancellous bone (AACB) could be modified by PVP to serve as sustained release carrier for bone growth factors. Bone morphogenetic protein (BMP) and basic fibroblast growth factor (bFGF) represent two well studied bone growth factors in recent years [5, 6]. The efficient osteoinductive activity of BMP has been proven in numerous experimental and clinical studies [7]. Meanwhile, bFGF has also been shown to be able to promote the osteogenesis induced by BMP, and stimulate the growth of capillaries [8-10]. However, recent studies about the effects of these two important growth factors in ANFH repairing have been mainly involving single applications.

In the present study, AACB was prepared out of dog vertebrae through decalcification, degreasing, and deproteinization, according to a previ-

ous method from our laboratory [11]. AACB was combined with BMP and bFGF, and then the AACB/BMP/bFGF complex artificial bone was implanted into dog ANFH models established by liquid nitrogen freezing method. Osteogenesis and angiogenesis was evaluated after implantation, and the feasibility of the AACB/BMP/bFGF complex in clinical use was discussed.

Materials and methods

AACB/BMP/bFGF complex preparation

AACB/BMP/bFGF complex was prepared by the Department of Orthopaedics, the First Affiliated Hospital of Kunming Medical College, as described previously [11]. Briefly, vertebral cancellous bone was harvested from 1-year dogs, and then subjected to degreasing with 1:1 chloroform/methanol for 12 h, deproteinization with 30% hydrogen peroxide for 48 h, and decalcification with 0.6 mmol/L hydrochloric acid for 2 min. AACB was obtained after the materials were freeze-dried at -50°C for 24 h, and then stored at 4°C.

Totally 300 mg BMP was dissolved in 10 ml guanidine hydrochloride solution with homogenization, and then dialyzed for 48 h (BMP was provided by the Institute of Orthopaedics, the Fourth Military Medical University, PLA, which has been proven by the mouse muscle pouch test to have osteoinductive activity).

Polyvinylpyrrolidone (PVP; 18 g) was mixed with 30 ml distilled water to make solution with certain viscosity, and used as release carriers for bFGF (15,000 units per package, provided by Essex Bio-Pharmaceutical Co., Ltd. Zhuhai, Guangdong, China). 12 g AACB was mixed with the PVP solution, and then divided into three aliquots (20 g each). One aliquot was mixed with 150 mg BMP solution, and another was mixed with both 16 μL bFGF solution (containing 24,000 IU bFGF) and 150 mg BMP solution. These mixtures were placed in 900-mmHg vacuum, at -40°C for vacuum suction and lyophilization. The complex was packaged under sterile conditions, and then stored at 4°C until further use.

Animal modeling

Models of femoral head necrosis were established as described by Yuekun Gong *et al.* [12]. Thirty healthy adult dogs, male or female, weighing 12.0 ± 1.9 kg, were provided by the Experimental Animal Center of Kunming Medical College. 3% (v/v) pentobarbital sodium was used for anesthesia through intravenous injection. Lateral hip incisions were made bilaterally to expose the femoral heads. Bone defect with a diameter of about 1 cm was created between femoral head and neck. Liquid nitrogen was maintained in the defect region for 1 min. The incisions were sutured after the defect area was treated with warm salt water.

At 8 w after modeling, through the same surgical approach, necrotic subchondral bone tissues were scraped until reaching the healthy red normal cancellous bone, forming bone defect with a diameter of 1.5 cm. These 30 dogs were then divided into 5 groups for implantation: Group A was the control group without any implantation; Group B was implanted with AACB; Group C was implanted with AACB/BMP; Group D was implanted with AACB/BMP/bFGF, and Group E was implanted with autologous cancellous bone (ilium). These dogs were sacrificed at 3 w, 6 w, and 12 w after implantation, respectively, for the following examinations and detections.

Anatomical observation

The diets, activities, and wound conditions were observed and recorded after implantation. After the dogs were sacrificed, femoral head samples were collected for the observation of collapse. Then the femoral heads were cut along the coronal plane, and the repairing processes were examined.

H & E staining

Femoral head samples were fixed with 10% (v/v) formaldehyde for 48 h, and then placed in EDTA solution for decalcification (solution changed weekly). When these samples become soft (about 5 w later), they were washed, dehydrated, and then embedded in paraffin. The samples were cut into 5 μm serial sections for H&E staining, and observed under microscope for bone formation.

The detection and analysis of bone formation were performed according to Thomopoulos *et al.* [13]. For the samples at 3 w, 6 w, and 12 w after implantation, three random fields of 100× magnification were selected in the defect region in each slice. According to the Delesse

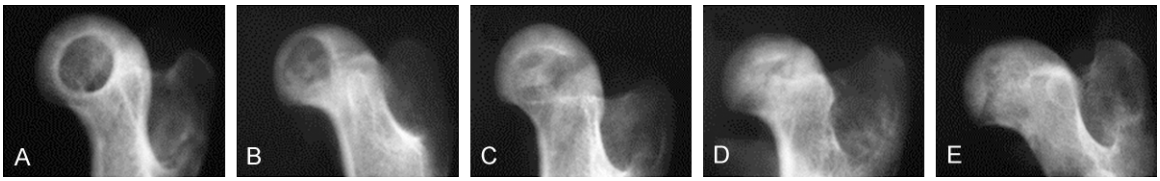

Figure 1. X-ray examination of the femoral heads in ANFH models at 12 w. A: Necrotic defect did not heal without any implantation (Group A); B: Bone density in the implanted region was lower than the surrounding bone tissue in the group implanted with AACB alone (Group B); C: Bone density was uneven in grafted areas in the group implanted with AACB/BMP (Group C); D: When implanted with AACB/BMP/bFGF complex (Group D), bone densities in the implanted region were comparable to the host bone area, and the boundary between these regions was indistinguishable, and similar results were observed in the group treated with autologous cancellous bone (Group E).

principle of stereology [13], the area percentage of a specific component in the entire profile area is a consistent estimate of the volume fraction of this component. HPIAS-1000, a high-resolution pathological image analysis system, was applied to observe the new born formation. The area percentage was then calculated according to the following formula: area percentage of new bone formation = new bone area/statistical field area (100×) × 100%.

Immunohistochemistry

CD_{34} monoclonal antibody (Maixin Reagent Company, Shanghai, China) was used for the immunohistochemical staining of femoral heads to detect the vascularization. Paraffin-embedded samples were cut into 4 μm serial sections, and the immunohistochemical staining was performed with the avidin-biotin-peroxidase complex (ABC) method. A distinct brown staining in the cytoplasm of endothelial cells was considered as positive. Three random fields of 100× magnification were selected in the defect area of each section, and the numbers of blood vessels were counted and calculated.

Statistical analysis

Data were expressed as mean ± SD. SPSS 11.5 statistical package was used for statistical analysis. ANOVA analysis was performed for comparison between groups. $P < 0.05$ was considered statistically significant.

Results

Anatomical observation of the femoral heads in ANFH models

All animal models behaved and started to eat on the very day of surgery, without inflammation at the incision site, femoral head dislocation and collapse, or femoral neck fracture. No death occurred as a result of the procedures. To evaluate the repairing effects of the implantations, anatomical observation of the femoral heads was performed at 3 w, 6 w, and 12 w after implantation. Our results indicated that, in the blank control group (Group A), at 12 w after operation, the defect area was always clearly distinguishable and filled with connective tissue. In the group implanted with AACB alone (Group B), sparse bone tissue was observed in the implanted region at 12 w. In the group implanted with AACB and BMP (Group C), newly generated bone tissues were found in the implanted region at 6 w after surgery, and incomplete bone remodeling was observed at 12 w. Moreover, in the group implanted with AACB/BMP/bFGF complex (Group D), at 3 w after operation, granulation tissue grew actively; at 6 w, the grafted complex was mostly absorbed, and there was plenty of new bone formation; at 12 w, bone remodeling was almost complete, and the boundary between grafts and host bone was blurred. In the group implanted with autologous cancellous bone (Group E), the grafts was absorbed, with moderate amount of newly generated bone tissues, at 6 w after surgery, and bone remodeling was complete at 12 w. These results suggest that the mixture of AACB/BMP/bFGF exerts the most efficient therapeutic effects in these dog ANFH models, compared with AACB alone and AACB plus BMP.

X-ray examination of the femoral heads in ANFH models

To further evaluate the effects of these grafts on the femoral heads in the ANFH models, X-ray examination was performed. At 3 w after sur-

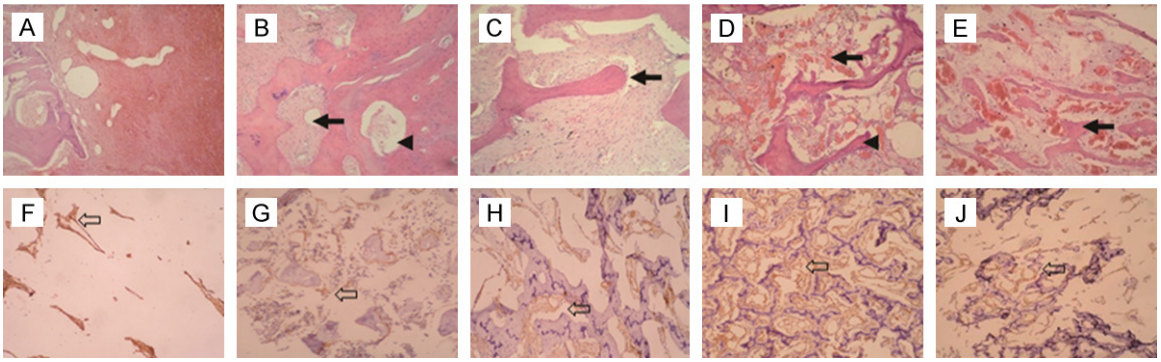

Figure 2. Histological observation and immunohistochemical staining. (A-E) Histological observation of new bone formation in ANFH models at 6 w. (A) In Group A, the defect region was mainly filled with connective tissues, loosely connected with host bone; (B) In Group B, limited new bone tissues were formed, and the grafts were incompletely absorbed (arrowhead); (C) In Group C, repairing processes were more effective and prevalent; (D) In Group D, the grafts were completely absorbed, and there were plenty of newly formed bone trabeculae and blood vessels (double arrowhead) in the implanted region; (E) In Group E, plenty of newly formed bone trabeculae were observed in the implanted region. Representative new bone formation was designated by arrows (H & E staining 100×). (F-J) Vascular immunohistochemical staining of the femoral heads in ANFH models at 3 w. The vascular densities were relatively low in Group A (F), B (G), and C (H), whereas the density was relatively high in Groups D (I) and E (J). Representative newly formed blood vessels were marked with open arrows in each group. (ABC method, 100×).

Table 1. Quantitative analysis of the newly formed bone area at 3 w, 6 w, and 12 w after implantation

	Group A	Group B	Group C	Group D	Group E
3 w	0.00 ± 0.00	0.00 ± 0.00	3.45 ± 1.28$^{*,\#}$	7.73 ± 1.15$^{*,\#,\&,\$}$	3.57 ± 1.27$^{*,\#}$
6 w	2.35 ± 1.14	4.79 ± 1.43	8.67 ± 1.34$^{*,\#}$	32.28 ± 2.17$^{*,\#,\&,\$}$	17.26 ± 1.20$^{*,\#,\&}$
12 w	4.52 ± 1.30	8.45 ± 1.01	33.73 ± 4.35$^{*,\#}$	37.3 ± 3.40$^{*,\#}$	40.40 ± 3.69$^{*,\#}$

Compared with Group A, $^{*}P < 0.05$; compared with Group B, $^{\#}P < 0.05$; compared with Group C, $^{\&}P < 0.05$; compared with Group E, $^{\$}P < 0.05$.

gery, no evidence of new bone generation was observed in Group A, while in all the other implanted groups, bone density in the implanted region was lower than the surrounding bone tissue. At 6 w, defect was clearly visible in Group A, while in other groups, the boundary between grafts and host bone started to be blurred. At 12 w after surgery, as shown in **Figure 1**, in Group A, defect did not heal; in Group B, bone density in the implanted region was lower than the surrounding bone tissue; in Group C, bone density was uneven in grafted areas; in both groups D and E, bone densities in the implanted region were comparable to the host bone area, and the boundaries between the implanted and surrounding regions were indistinguishable. These results further confirm that AACB/BMP/bFGF complex could effectively repair the injuries in these dog ANFH models, almost to a comparable level with cancellous bone autografts.

Histological observation of the newly formed bone tissues in ANFH models

New bone formation is one of the important indicators for ANFH repairing. So the newly generated bone tissues were investigated in these ANFH models with H & E staining (**Figure 2A-E**). Our results indicated that, in the control group (Group A), the defect region was mainly filled with the connective tissue all the time, which was loosely connected with host bone tissues. On the other hand, there were obvious differences between the other implanted groups. At 3 w after operation, in Group C, sporadic bone precursor cells and osteoblasts were found in the implanted region. In Group D, active new bone formation (as indicated by the large amount of bone precursor cells and osteoblasts), as well as angiogenesis, were observed. At 6 w, as shown in **Figure 2A-E**, the grafts were incompletely absorbed, and limited new bone tissues were formed in Group B, while the repairing processes were more effective and prevalent in Group C. In Group D, the grafts were completely absorbed, and there were plenty of newly formed bone trabeculae

Table 2. Numbers of blood vessels at 3 w and 6 w after implantation

	Group A	Group B	Group C	Group D	Group E
3 w	1.75 ± 0.50	3.25 ± 0.96*	3.75 ± 0.50*	7.75 ± 0.96*,#,&,$	4.25 ± 0.50*,#
6 w	2.50 ± 0.58	4.25 ± 0.96*	5.75 ± 0.96*	11.00 ± 1.63*,#,&,$	8.00 ± 0.82*,#,&

Compared with Group A, *P < 0.05; compared with Group B, #P < 0.05; compared with Group C, &P < 0.05; compared with Group E, $P < 0.05.

and blood vessels in the implanted region. Similar results were also seen in Group E. At 12 w, the bone densities were uneven in the defect area in Group B, and the bone remodeling processes were not complete in Group C. In Groups D and E, however, the bone remodeling processes were as good as the normal cancellous bone.

As shown in **Table 1**, further quantitative bone measurement indicated that, at 3 w after operation, significantly more new bone tissues were formed in Group D (7.73 ± 1.15%), as compared with Groups C and E, where lower levels of bone formation were observed (P < 0.05). At 6 w, 32.28 ± 2.17% newly generated bone tissues were detected in Group D, which was still superior to any of the other implanted groups (P < 0.05). While at 12 w after implantation, there were significantly more new bone tissues in Group D (37.30 ± 3.40%) than Groups A and B (P < 0.05). However, no significant differences were observed in the relative amount of newly formed bone between Groups D, C, and E (P > 0.05). Taken together, these results suggest that AACB/BMP/bFGF complex could enhance new bone formation to contribute to the healing of ANFH.

Vascular immunohistochemical staining of the femoral heads in ANFH models

Angiogenesis is another important aspect of the healing of femoral head necrosis, especially ANFH. To further evaluate the therapeutic effects of these grafts on AMFH, vascular immunohistochemical staining and the subsequent quantitative analysis were carried out (**Figure 2F-J**; **Table 2**). Our results showed that, at 3 w after implantation, the lowest number of vessels was in Group A (1.75 ± 0.50), and highest was in Group D (7.75 ± 0.96), both significantly different from other groups (P < 0.05). Similar results were observed at 6 w after surgery. Groups A and D made the lowest and the highest number of vessels (2.50 ± 0.58 for Group A, and 11.00 ± 1.63 for Group D), respectively, which were significantly different from the other groups (P < 0.05). These results suggest that AACB/BMP/bFGF complex could significantly stimulate the revascularization in the defect areas, contributing to the post-injury healing process in ANFH models.

Discussion

To date, there is still not a generally accepted method that can be used to treat adult ANFH. Bone growth factors have been shown to be able to promote bone formation and angiogenesis, offering a breakthrough for the improvement of the ANFH therapy [5]. It has been shown that polyvinylpyrrolidone (PVP), when mixed with distilled water to make solution with certain viscosity, could be used as a controlled release carrier for bFGF [3]. Moreover, AACB can be used not only as scaffold materials, but also as a BMP carrier. In the present study, PVP, AACB, bFGF, and BMP were mixed by a certain percentage, to obtain AACB/BMP/bFGF complex artificial bone [11, 14], which was transplanted into the dog ANFH models through fenestration/decompression. Our results indicated that implantation of the complex significantly promoted the angiogenesis and osteogenesis by releasing of bFGF and BMP, contributing to the repair of ANFH defect.

For the study of graft treatment for ANFH, animal models could be established by the graft implantation procedures after removing the sequestrum and surgical fenestration/decompression, rather than simply mimicking the etiology and pathogenesis of the disease [15-18]. Our results showed that femoral head defect and necrosis started to appear only three days after surgery, and bone repair gradually stopped without any treatment [12]. Eight weeks after modeling, through the same surgical approach, necrotic subchondral bone tissues were scraped, reaching the healthy red normal cancellous bone. The bone defect with 1.5 cm diameter would not self-heal at 12 w (Group A), indicating our modeling method was suitable for the study of the disease. On the other hand, the articular cartilage fragmentation and the collapse of femoral heads were not observed,

probably due to the fact that these model dogs were housed in cages, with less heavy burden and walking. To this end, the AMFH models should be modified to investigate the specific functions of AACB/BMP/bFGF complex in preventing the articular cartilage fragmentation and the collapse of femoral heads.

Ideal bone graft material should be easily absorbed and degraded, with good histocompatibility [19]. In Group B implanted with AACB, the materials were degraded and absorbed at 12 w, just as natural cancellous bone, without obvious inflammation and lymphocyte infiltration in histological sections. Six weeks after AACB implantation, new bone tissues begun to form, although with uneven maturity, indicating that the performance of this material alone is insufficient to repair the defect in femoral heads. When mixed with BMP, an osteoinductive growth factors [5, 20], AACB/BMP complex transplantation (Group B) showed dramatically higher osteogenic capability than Group C. At 3 w after implantation, there were osteoblast precursor cells and osteoblasts, and at 6 w, new bone formation started. However, at 12 w, the bone remodeling has not been completed, indicating the combination of AACB and BMP is still not enough to fix the defect in this particular part of femoral heads.

Osteoinduction and bone formation involve various growth factors and regulators [21]. The bFGF has been shown to be able to promote the bone maturation and cartilage cell proliferation, and stimulate the secretion of other growth factors. Furthermore, bFGF is also a potent angiogenic growth factor [20]. In our experiments, PVP was used as a soluble carrier for bFGF, and then mixed with BMP and AACB to form AACB/BMP/bFGF complex artificial bone. Results from histology and immunohistochemistry showed that this AACB/BMP/bFGF complex was superior to the materials used in Group C in inducing osteogenesis and angiogenesis. These effects might be attributed to the fact that bFGF could improve the cartilage cell proliferation, and stimulate other growth factors to induce angiogenesis. Moreover, the undifferentiated mesenchymal stem cells could thereby enhance osteogenesis by BMP induction.

Autologous bone graft is known as the gold standard for bone graft [22]. The X-ray detection indicated that, in Group D (implanted with AACB/BMP/bFGF complex) and Group E (grafted with autologous cancellous bone), at 12 w after implantation, the bone densities in the implanted area were similar as the host bone, with blurred boundaries. Meanwhile, the anatomical observation and histochemical detection indicated that, in Groups D and E, bone remodeling was comparable to normal cancellous bone, without significant differences between these two groups. However, at early time in bone repairing (such as at 3 w or 6 w), the amounts of new blood vessels and new bone formation in Group D was significantly more than Group E, suggesting that AACB/BMP/bFGF complex is more effective in inducing revascularization and osteogenesis, compared with autologous cancellous bone grafts.

In conclusion, AACB/BMP/bFGF complex artificial bone could repair the defect in femoral head necrosis models, with rapid and sufficient effects. The efficacy of AACB/BMP/bFGF complex was comparable or even superior, in some aspects, to that of autologous cancellous bone grafts. When the safety has been further confirmed, AACB/BMP/bFGF complex would be widely used in clinical applications for ANFH treatment.

Acknowledgements

This work was supported by the joint fund from the Science and Technology Department of Guizhou Province and Guiyang Medical College (Guizhou S&T cooperation [2010] 3165), the S&T fund from the Health Department of Guizhou Province (gzwkj2010-1-039), and the Science and Technology Fund Project of Guizhou Province (Guizhou S&T cooperation J [2013]2038).

Disclosure of conflict of interest

None.

Address correspondence to: Wuxun Peng, Department of Emergency Surgery, Guiyang Medical College Hospital, Guiyi Street, Guiyang 550004, China. Tel: 86-139 8486 3732; E-mail: pengwuxun1971@163.com

References

[1] Liang HY, Huang NN, Tang Q, Chen JH, Xiao F. Primary study of SGBG/PHBV applying to scaf-

fold material of periodontal tissue engineering. China Journal of Modern Medicine 2008; 18: 1793-1796.
[2] Ji Y, Xu GP, Zhang ZP, Xia JJ, Yan JL, Pan SH. BMP-2/PLGA delayed-release microspheres composite graft, selection of bone particulate diameters, and prevention of aseptic inflammation for bone tissue engineering. Ann Biomed Eng 2010; 38: 632-639.
[3] Bharali DJ, Sahoo SK, Mozumdar S, Maitra A. Cross-linked polyvinylpyrrolidone nanoparticles: a potential carrier for hydrophilic drugs. J Colloid Interface Sci 2003; 258: 415-423.
[4] Gorskaya UF, Danilova TA, Mezentzeva MV, Shapoval MM, Nesterenko VG. Effect of immunization with polyvinylpyrrolidone on the counts of stromal precursor cells in bone marrow and spleen of CBA and CBA/N mice and cytokine gene expression in primary cultures of these cells. Bull Exp Biol Med 2012; 153: 64-67.
[5] Wang L, Huang Y, Pan K, Jiang X, Liu C. Osteogenic responses to different concentrations/ratios of BMP-2 and bFGF in bone formation. Ann Biomed Eng 2010; 38: 77-87.
[6] Varkey M, Kucharski C, Haque T, Sebald W, Uludağ H. In vitro osteogenic response of rat bone marrow cells to bFGF and BMP-2 treatments. Clin Orthop Relat Res 2006; 443: 113-123.
[7] Chen B, Lin H, Wang J, Zhao Y, Wang B, Zhao W, Sun W, Dai J. Homogeneous osteogenesis and bone regeneration by demineralized bone matrix loading with collagen-targeting bone morphogenetic protein-2. Biomaterials 2007; 28: 1027-1035.
[8] Nakamura S, Nambu M, Ishizuka T, Hattori H, Kanatani Y, Takase B, Kishimoto S, Amano Y, Aoki H, Kiyosawa T, Ishihara M, Maehara T. Effect of controlled release of fibroblast growth factor-2 from chitosan/fucoidan micro complex-hydrogel on in vitro and in vivo vascularization. J Biomed Mater Res A 2008; 85: 619-627.
[9] Yuan S, Pan Q, Fu CJ, Bi Z. Effect of growth factors (BMP-4/7 & bFGF) on proliferation & osteogenic differentiation of bone marrow stromal cells. Indian J Med Res 2013; 138: 104-110.
[10] Zhao YZ, Tian XQ, Zhang M, Cai L, Ru A, Sheng XT, Jiang X, Jin RR, Zheng L, Hawkins K, Charkrabarti S, Li XK, Lin Q, Yu WZ, Ge S, Lu CT, Wong HL. Functional and pathological improvements of the hearts in diabetes model by the combined therapy of bFGF-loaded nanoparticles with ultrasound-targeted microbubble destruction. J Control Release 2014; 186: 22-31.
[11] Peng WX, Gong YK, Li SH. Experimental study on procedures and properties of composite derived material of heterogeneous bone. Medicine and Pharmacy of Yunnan 2004; 25: 458-460.
[12] Gong YK, Peng WX, Li SH, Wang X, Li XH. Bone defect and necrosis of the femoral head produced in canines by freezing: an experimental study. The Orthopedic Journal of China 2005; 13: 1171-1173.
[13] Thomopoulos S, Harwood FL, Silva MJ, Amiel D, Gelberman RH. Effect of several growth factors on canine flexor tendon fibroblast proliferation and collagen synthesis in vitro. J Hand Surg Am 2005; 30: 441-447.
[14] Xu L, Zhi-Ming Y, Xue-Mei L. An experimental study of bioderived bone to repair bone defect as a scaffold of tissue engineering. Int Surg 2008; 93: 377-380.
[15] Mont MA, Jones LC, Elias JJ, Inoue N, Yoon TR, Chao EY, Hungerford DS. Strut-autografting with and without osteogenic protein-1: A preliminary study of a cavine femoral head defect model. J Bone Joint Surg Am 2001; 83: 1013-1022.
[16] Sun J, Hou XK, Li X, Tang TT, Zhang RM, Kuang Y, Shi M. Mosaicplasty associated with gene enhanced tissue engineering for the treatment of acute osteochondral defect in a goat model. Arch Orthop Trauma Surg 2009; 129: 757-771.
[17] Wen Q, Ma L, Chen YP, Yang L, Luo W, Wang XN. A rabbit model of hormone-induced early avascular necrosis of the femoral head. Biomed Environ Sci 2008; 21: 398-403.
[18] Kerachian MA, Cournoyer D, Harvey EJ, Chow TY, Bégin LR, Nahal A, Séguin C. New insights into the pathogenesis of glucocorticoid-induced avascular necrosis: microarray analysis of gene expression in a rat model. Arthritis Res Ther 2010; 12: R124.
[19] Cao K, Huang W, An H, Jiang DM, Shu Y, Han ZM. Deproteinized bone with VEGF gene transfer to facilitate the repair of early avascular necrosis of femoral head of rabbit. Chin J Traumatol 2009; 12: 269-274.
[20] Stewart K, Pabbruwe M, Dickinson S, Sims T, Hollander AP, Chaudhuri JB. The effect of growth factor treatment on meniscal chondrocyte proliferation and differentiation on polyglycolic acid scaffolds. Tissue Eng 2007; 13: 271-280.
[21] Shi YH, Bingle L, Gong LH, Wang YX, Corke KP, Fang WG. Basic FGF augments hypoxia induced HIF-1-alpha expression and VEGF release in T47D breast cancer cells. Pathology 2007; 39: 396-400.
[22] Sbordone L, Toti P, Menchini-Fabris G, Sbordone C, Guidetti F. Implant survival in maxillary and mandibular osseous onlay grafts and native bone: a 3-year clinical and computerized tomographic follow-up. Int J Oral Maxillofac Implants 2009; 24: 695-703.